Soft Matter

COMMUNICATION

View Article Online
View Journal

Cite this: DOI: 10.1039/d1sm01221e

Received 20th August 2021,
Accepted 6th September 2021

DOI: 10.1039/d1sm01221e

rsc.li/soft-matter-journal

Phosphobisaromatic motifs enable rapid enzymatic self-assembly and hydrogelation of short peptides†

Meihui Yi,[a] Jiaqi Guo,[a] Hongjian He,[a] Weiyi Tan,[a] Nya Harmon,[b] Kesete Ghebreyessus[b] and Bing Xu*[a]

Enzyme-instructed self-assembly (EISA) and hydrogelation is a versatile approach for generating soft materials. Most of the substrates for alkaline phosphatase catalysed EISA utilize phosphotyrosine ($_p$Tyr) as the enzymatic trigger for EISA and hydrogelation. Here we show the first example of phosphonaphthyl ($_p$NP) and phosphobiphenyl ($_p$BP) motifs acting as faster enzymatic triggers than phosphotyrosine for EISA and hydrogelation. This work illustrates novel enzyme triggers for rapid enzymatic self-assembly and hydrogelation.

Enzyme-instructed self-assembly (EISA) or enzymatic noncovalent synthesis,[1] as a versatile approach for mimicking the regulation of noncovalent interactions of biomolecules in a living cell, has emerged as a useful bottom-up strategy for controlling functional supramolecular peptide assemblies,[2] which promise a wide range of potential applications of soft materials in biomedicine, such as tissue engineering,[3,4] molecular imaging,[5–7] drug delivery,[8–10] multimolecular crowding in biosystems,[11] and cancer therapy.[12–16] Because enzymatic reactions provide a fast and specific transformation of supramolecular peptide assemblies, EISA is particularly attractive for generating non-diffusive supramolecular assemblies[17–19] in the cellular environment[20] for modulating cellular activities,[21] such as apoptosis,[22] morphogenesis,[23] and protein trafficking.[24,25] Most of these studies related to short peptides utilize phosphotyrosine ($_p$Tyr) as an enzymatic trigger[26] being activated by alkaline phosphatase (ALP) for initiating self-assembly of the peptides because ALP plays important roles in cell biology and is overexpressed in certain tumours.[27,28] Particularly, most of these peptides contain an aromatic capping motif, such as the naphthyl,[29] fluorenyl,[30] or pyrenyl[31] group, at the N-terminal and L- or D-$_p$Tyr at the C-terminal or in the middle of the peptides.[31–34] A representative example of EISA substrates is Nap-ff$_p$y (**1P**), which carries a D-$_p$Tyr ($_p$y) at the C-terminal of the peptide. **1P** has revealed many key features of EISA and led to unexpected formation of pericellular nanofibers that selectively kill cancer cells.[35] On the other hand, the phosphate trigger at the N-terminal of the peptide is much less explored, except the work of Ye *et al.* that employs a phosphorylated dye at the N-terminal of a peptide,[7] but the rate of dephosphorylation is relatively slow.

Therefore, we decide to examine the dephosphorylation of an N-terminal aromatic capping motif of short peptides for enzymatic self-assembly and hydrogelation. As shown in Scheme 1, we attach phosphohydroxybenzoic acid ($_p$B), phosphohydroxynaphthoic acid ($_p$NP), or phosphohydroxybiphenylcarboxylic acid ($_p$BP) at the N-terminal of the D-diphenylalanine (ff)[36] or D-tri-phenylalanine peptide (fff) to generate phosphorylated peptide derivatives (**2-7P**) as the substrates of ALP. Our results show that while the ff derivatives are unable to form hydrogels, the fff derivatives result in hydrogels after ALP-catalysed

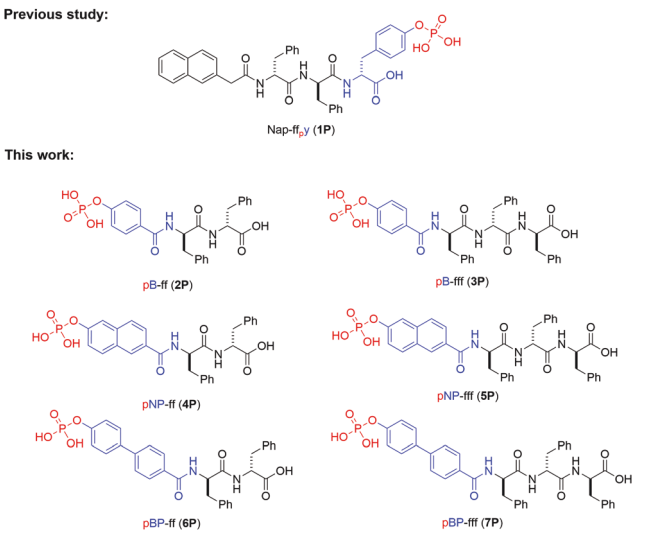

Scheme 1 Structures of the peptide derivatives with phosphate at the C-terminal (previously explored) and N-terminal (this work).

[a] Department of Chemistry, Brandeis University, 415 South Street, Waltham, MA, 02453, USA. E-mail: bxu@brandeis.edu
[b] Department of Chemistry and Biochemistry, Hampton University, Hampton, VA, 23668, USA

† Electronic supplementary information (ESI) available. See DOI: 10.1039/d1sm01221e

dephosphorylation converting the nanoparticles made of the precursors to nanofibers consisting of the corresponding hydrogelators (*i.e.*, **3**, **5**, or **7**). Rheological evaluation shows that the resulting three hydrogels have relatively high storage moduli, up to 10^4 Pa, when the concentrations of the hydrogelators are about 8 mM (about 0.5 wt%). Moreover, $_p$BP and $_p$NP act as faster enzyme triggers than the $_p$y and $_p$B motif for hydrogelation. As the first example to show the dephosphorylation of $_p$BP and $_p$NP for rapid enzymatic self-assembly and hydrogelation, this work offers a novel molecular platform and identifies fast triggers for EISA catalysed by ALP.

Scheme 1 shows the structures of the designed substrates of ALP. Based on the structure of **1P**, we use $_p$B, $_p$NP or $_p$BP as the enzymatic trigger of ALP to replace $_p$y in **1P**. We also move the ALP trigger to the N-terminal of the peptides. That is, $_p$B, $_p$NP or $_p$BP acts as the N-terminal capping group for ff or fff. Such a combination leads to six substrates of ALP: $_p$B-ff (**2P**), $_p$B-fff (**3P**), $_p$NP-ff (**4P**), $_p$NP-fff (**5P**), $_p$BP-ff (**6P**), and $_p$BP-fff (**7P**). After being dephosphorylated by ALP, these substrates would result in six peptide derivatives: B-ff (**2**), B-fff (**3**), NP-ff (**4**), NP-fff (**5**), BP-ff (**6**), and BP-fff (**7**). According to this design, we first produce $_p$B, $_p$NP and $_p$BP according to previously reported procedures.[37] Then, we, using Fmoc-based solid-phase peptide synthesis,[38] synthesize the six substrates of ALP.

After obtaining the precursors, we examine enzymatic gelation of these substrates upon the addition of ALP. Each precursor dissolves in PBS buffer to form a clear solution with a concentration of 0.5 wt%. As shown in Fig. 1, enzymatic dephosphorylation of **3P**, **5P** or **7P** results in a hydrogel 24 h after adding ALP. While the dephosphorylation of **2P** and **4P** affords a solution, the dephosphorylation of **6P** results in a suspension. This result indicates that **2** or **4** is more water soluble than **6**, agreeing with the higher hydrophobicity of biphenyl ($\log P$ = 3.71) than those of the naphthyl ($\log P$ = 3.03) and phenyl ($\log P$ = 2.03) groups. These results also suggest that the tri-phenylalanine enhances intermolecular interactions to favour hydrogelation of **3**, **5**, or **7**.

We use a dynamic time sweep to characterize the rheological properties of the hydrogels resulting from EISA of **3P**, **5P**, and **7P** by measuring their storage and loss moduli (G' and G'') (Fig. 2). We make solutions of **3P**, **5P**, and **7P** with concentrations of 8 mM (about 0.5 wt%). After the addition of ALP to the solution of **3P**, a crossover of G' and G'' occurs at about 1 h or 11 h of incubation when the concentration of ALP is 1.0 or 0.1 U mL^{-1}, respectively. With the treatment of 1.0 U mL^{-1} or 0.1 U mL^{-1} ALP, the solution of **5P** shows the crossover of G' and G'' at around 2 minutes or at 20 minutes, respectively. Being incubated with ALP at 1.0 or 0.1 U mL^{-1}, the solution of **7P** exhibits the crossover of G' and G'' at less than one minute or at about 13 minutes, respectively. These results indicate that $_p$BP or $_p$NP, as an enzyme trigger, enables enzymatic hydrogelation about 50–60 times faster than $_p$B does. Moreover, the times of **5P** and **7P** to reach the gelation point are two and three times shorter than that of **1P** (Fig. S1, ESI†), respectively. This result confirms that $_p$BP and $_p$NP are faster enzyme triggers for EISA than $_p$y. After 12 hours, the G' values of the hydrogels by EISA of **3P**, **5P**, and **7P** reach their plateau values when the concentration of ALP is 1.0 U mL^{-1}.

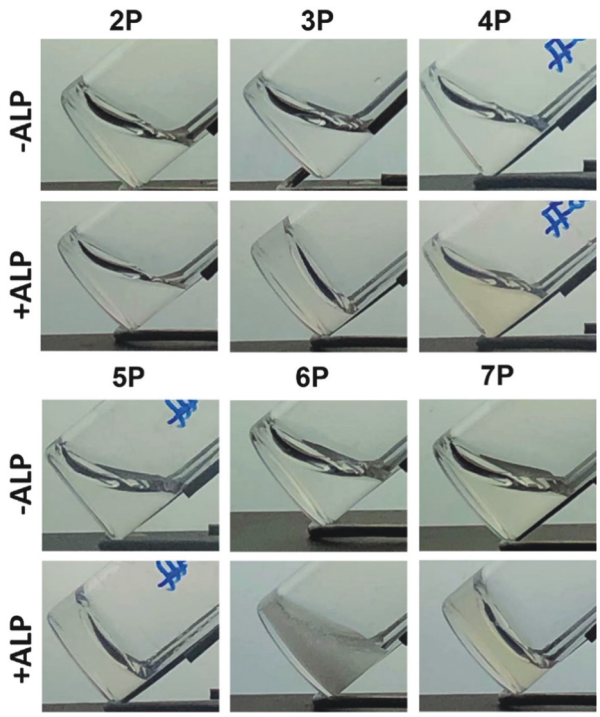

Fig. 1 The optical images of **2P**, **3P**, **4P**, **5P**, **6P** and **7P** (0.5 wt% in PBS buffer, pH 7.4) before and after incubation with ALP (1 U mL^{-1}) for 24 h.

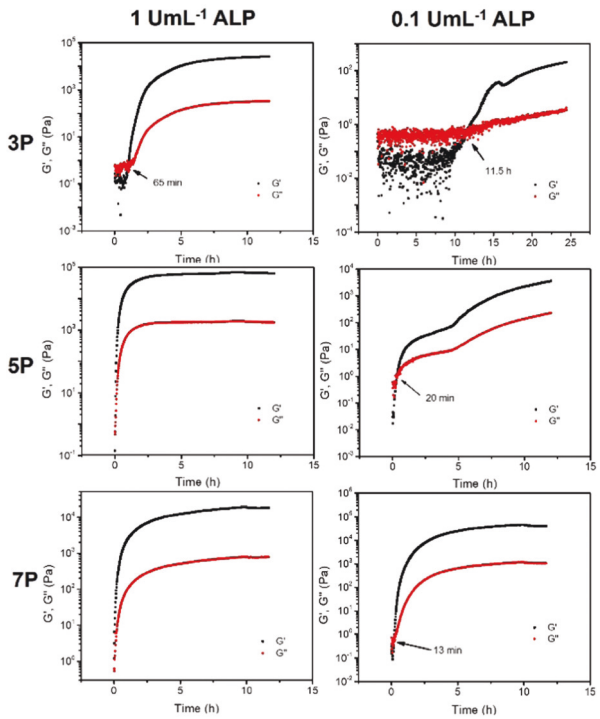

Fig. 2 Dynamic time sweeps of **3P** (8 mM), **5P** (8 mM), and **7P** (8 mM) incubated with ALP at 1 and 0.1 U mL^{-1} and at a strain of 1% and frequency of 6.28 rad s^{-1}.

We also conduct frequency and strain sweeps (Fig. 3) of the hydrogels. The strain and frequency applied in the time sweep fall within the linear viscoelastic range of the gels, indicating that the time-dependent strain sweeps are carried out under appropriate conditions. Being incubated with 1 U mL^{-1} and 0.1 U mL^{-1} of ALP, the hydrogels, being made of **3**, **5**, or **7**, obtained by the dephosphorylation of **3P**, **5P**, or **7P**, exhibit a frequency-independent G' (0.1 rad s^{-1} to 200 rad s^{-1}), suggesting that the gels behave as solid-like. For the gel resulting from dephosphorylation of **3P** by 1 U mL^{-1} of ALP, G' and G'' are independent of the strain below 1% and show the existence of a linear viscoelastic region (LVR). Within the LVR, G' (up to 10^4 Pa) is significantly greater than G'', reflecting the dominant elastic nature. For the gel resulting from dephosphorylation of **3P** by 0.1 U mL^{-1} of ALP, though $G' > G''$ below 1% strain, G'' fluctuates and increases with the increase of the strain, which fails to show an LVR and indicates the hydrogel being relatively weak. Unlike the case of **3P**, the strain sweeps of the hydrogels resulting from dephosphorylation of **5P** or **7P** by 1 or 0.1 U mL^{-1} of ALP show that G' and G'' are independent of the strain below 2%. Both show the existence of a linear viscoelastic region (LVR), suggesting that NP or BP enhances the viscoelasticity of the hydrogels made of **5** or **7**.

To investigate the morphological properties, we use transmission electron microscopy (TEM) to image these precursors without or with the addition of ALP. As shown in Fig. 4, TEM of the solutions of **2P**, **4P**, **6P**, and **7P** shows aggregated nanoparticles, with diameters about 10 nm. While the TEM of the solution of **3P** reveals the existence of short nanofibers with diameters of 4 nm, the TEM of the solutions of **5P** shows the coexistence of short nanofibers with diameters of 4 nm and nanoparticles. After the addition of 0.1 U mL^{-1} of ALP into the solutions of **2P** and **6P** for 24 h, the resulting solutions of **2** and the suspension of **6** contain nanoparticles with diameters around 12 nm. The resulting solution of **4** showed the coexistence of nanoparticles and nanosheets. The hydrogels of **3** show extended and entangled nanofibers with diameters of 4 nm, and some of the nanofibers form bundles with a diameter of 14 nm; the hydrogel of **5** shows uniform nanofibers with a width of 8 nm; and the hydrogel of **7** shows uniform bundles with a diameter of 13 ± 2 nm. The formation of the nanofibers of **3**, **5**, or **7** likely contributes to the formation of the hydrogel of **3**, **5**, or **7**. Notably, while the scanning electron microscopy (SEM) image of the dried gel of **3** displays nanofiber networks, the dried gel of **7** is largely amorphous with a few thick fibres (Fig. S2, ESI†), agreeing with the high hydrophobicity of the biphenyl group significantly enhancing the intermolecular interactions of **7**.

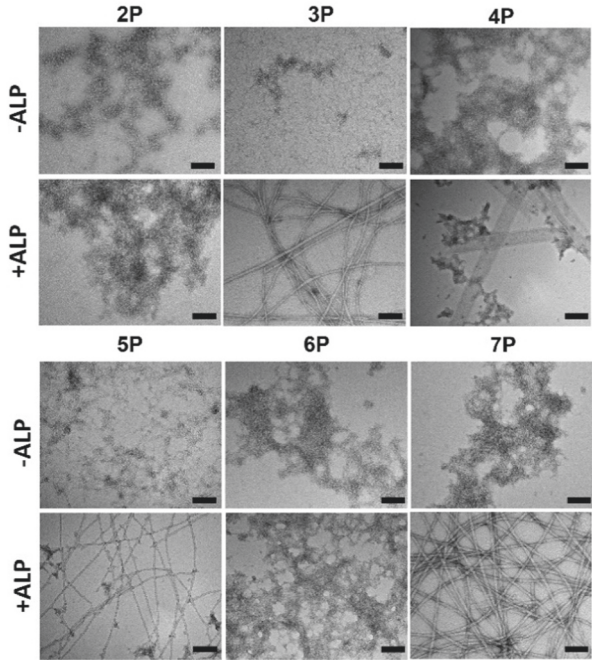

Fig. 4 The TEM images of **2P**, **3P**, **4P**, **5P**, **6P** and **7P** at 8 mM before and after ALP treatment. The concentration of ALP is 0.1 U mL^{-1}. The duration time is 24 h. The scale bar is 100 nm.

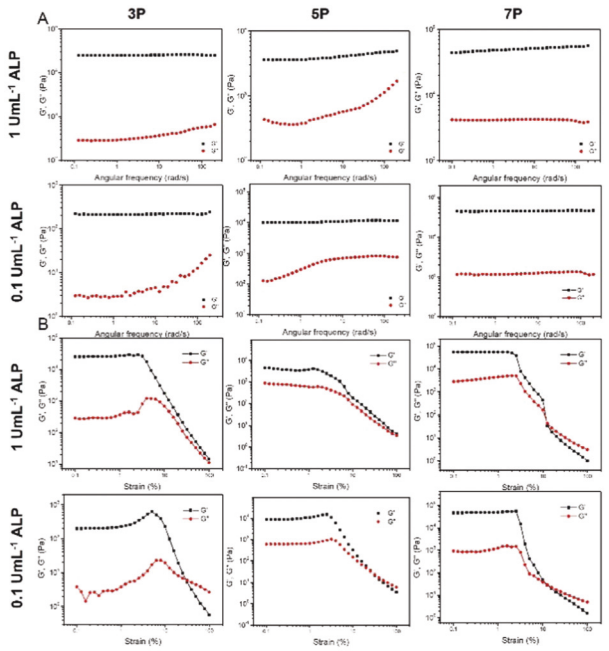

Fig. 3 (A) Frequency sweeps of **3P** (8 mM), **5P** (8mM), and **7P** (8 mM) conducted after 24 h incubation with ALP at 1.0 and 0.1 U mL^{-1} and at a strain of 1%. (B) Dynamic strain sweeps of **3P** (8 mM), **5P** (8 mM), and **7P** (8 mM) conducted after 24 h incubation with ALP at 1.0 and 0.1 U mL^{-1} and at a frequency of 6.28 rad s^{-1}.

In summary, we design six short peptides, containing phosphoaromatic that is both the N-terminal capping group and the enzyme trigger, as novel ALP substrates for EISA and hydrogelation. The ability to form hydrogels indicates that the tripeptide backbone having aromatic groups (*i.e.*, Phe and/or Tyr) enhances self-assembly and leads to hydrogelation. The result that $_p$BP is a faster substrate than $_p$Tyr for ALP agrees with the report that $_p$BP is a faster substrate than $_p$Tyr for protein tyrosine phosphatase 1 (PTP1B).[39] The rates of enzymatic hydrogelation catalysed by ALP follow the trend of **7P** > **5P** > **1P** > **3P**, implying that distancing the phosphate trigger

away from the peptide backbone likely favours fast enzymatic self-assembly, a design principle that may help combine EISA with other self-assembling molecules.[40–49] This work also suggests that it is worthwhile to examine other phosphobisaromatic capping groups for exploring anticancer drug candidates that act *via* EISA catalysed by phosphatases.

Conflicts of interest

There are no conflicts to declare.

Acknowledgements

This work was partially supported by the NIH (CA142746, CA252364) and NSF (DMR-2011846 and PREM-1827820).

References

1 H. He, W. Tan, J. Guo, M. Yi, A. N. Shy and B. Xu, *Chem. Rev.*, 2020, **120**, 9994.
2 B. J. Kim and B. Xu, *Bioconjugate Chem.*, 2020, **31**, 492.
3 H. Cui, M. J. Webber and S. I. Stupp, *Pept. Sci.*, 2010, **94**, 1.
4 Y. Shang, Z. Wang, R. Zhang, X. Li, S. Zhang, J. Gao, X. Li and Z. Yang, *Chem. Commun.*, 2019, **55**, 5123.
5 Z. Hai and G. Liang, *Adv. Biosyst.*, 2018, **2**, 1800108.
6 Y. He, J. Yu, X. Hu, S. Huang, L. Cai, L. Yang, H. Zhang, Y. Jiang, Y. Jia and H. Sun, *Chem. Commun.*, 2020, **56**, 13323.
7 R. Yan, Y. Hu, F. Liu, S. Wei, D. Fang, A. J. Shuhendler, H. Liu, H.-Y. Chen and D. Ye, *J. Am. Chem. Soc.*, 2019, **141**, 10331.
8 L. Mei, S. He, Z. Liu, K. Xu and W. Zhong, *Chem. Commun.*, 2019, **55**, 4411.
9 Y. Shi, Z. Wang, X. Zhang, T. Xu, S. Ji, D. Ding, Z. Yang and L. Wang, *Chem. Commun.*, 2015, **51**, 15265.
10 Y. Wang, A. G. Cheetham, G. Angacian, H. Su, L. Xie and H. Cui, *Adv. Drug Delivery Rev.*, 2017, **110–111**, 112.
11 Z. Feng, H. Wang and B. Xu, *J. Am. Chem. Soc.*, 2018, **140**, 16433.
12 Z. Feng, X. Han, H. Wang, T. Tang and B. Xu, *Chem*, 2019, **5**, 2442.
13 M. T. Jeena, S. Lee, A. K. Barui, S. Jin, Y. Cho, S.-W. Hwang, S. Kim and J.-H. Ryu, *Chem. Commun.*, 2020, **56**, 6265.
14 A. Tanaka, Y. Fukuoka, Y. Morimoto, T. Honjo, D. Koda, M. Goto and T. Maruyama, *J. Am. Chem. Soc.*, 2015, **137**, 770.
15 Q. Yao, F. Lin, X. Fan, Y. Wang, Y. Liu, Z. Liu, X. Jiang, P. R. Chen and Y. Gao, *Nat. Commun.*, 2018, **9**, 5032.
16 Z. M. Yang, K. M. Xu, Z. F. Guo, Z. H. Guo and B. Xu, *Adv. Mater.*, 2007, **19**, 3152.
17 M. P. Hendricks, K. Sato, L. C. Palmer and S. I. Stupp, *Acc. Chem. Res.*, 2017, **50**, 2440.
18 D. Ivnitski, M. Amit, O. Silberbush, Y. Atsmon-Raz, J. Nanda, R. Cohen-Luria, Y. Miller, G. Ashkenasy and N. Ashkenasy, *Angew. Chem., Int. Ed.*, 2016, **55**, 9988.
19 G. Ouyang and M. Liu, *Mater. Chem. Front.*, 2020, **4**, 155.
20 Z. Feng, H. Wang, F. Wang, Y. Oh, C. Berciu, Q. Cui, E. H. Egelman and B. Xu, *Cell Rep. Phys. Sci.*, 2020, **1**, 100085.
21 J. Zhan, J. Zhong, S. Ma, W. Ma, Y. Wang, Z. Yu, Y. Cai and W. Huang, *Chem. Commun.*, 2020, **56**, 6957.
22 X. Du, J. Zhou, H. Wang, J. Shi, Y. Kuang, W. Zeng, Z. Yang and B. Xu, *Cell Death Dis.*, 2017, **8**, e2614.
23 J. Zhou, X. Du, X. Chen and B. Xu, *Biochemistry*, 2018, **57**, 4867.
24 H. He, J. Guo, J. Xu, J. Wang, S. Liu and B. Xu, *Nano Lett.*, 2021, **9**, 4078.
25 D. Yang, H. He, B. J. Kim and B. Xu, *Bioconjugate Chem.*, 2021, **3**, 502.
26 Z. Yang, H. Gu, D. Fu, P. Gao, J. K. Lam and B. Xu, *Adv. Mater.*, 2004, **16**, 1440.
27 W. H. Fishman, N. R. Inglis, S. Green, C. L. Anstiss, N. K. Gosh, A. E. Reif, R. Rustigian, M. J. Krant and L. L. Stolbach, *Nature*, 1968, **219**, 697.
28 P. H. Lange, J. L. Millan, T. Stigbrand, R. L. Vessella, E. Ruoslahti and W. H. Fishman, *Cancer Res.*, 1982, **42**, 3244.
29 J. Shi, X. Du, D. Yuan, J. Zhou, N. Zhou, Y. Huang and B. Xu, *Biomacromolecules*, 2014, **15**, 3559.
30 J. Gao, H. Wang, L. Wang, J. Wang, D. Kong and Z. Yang, *J. Am. Chem. Soc.*, 2009, **131**, 11286.
31 J. Li, Z. Zhan, X. Du, J. Wang, B. Hong and B. Xu, *Angew. Chem., Int. Ed.*, 2018, **57**, 11716.
32 H. Wang, C. Yang, M. Tan, L. Wang, D. Kong and Z. Yang, *Soft Matter*, 2011, **7**, 3897.
33 Q. Yao, C. Wang, M. Fu, L. Dai, J. Li and Y. Gao, *ACS Nano*, 2020, **14**, 4882.
34 Z. Zheng, P. Chen, M. Xie, C. Wu, Y. Luo, W. Wang, J. Jiang and G. Liang, *J. Am. Chem. Soc.*, 2016, **138**, 11128.
35 Y. Kuang, J. Shi, J. Li, D. Yuan, K. A. Alberti, Q. Xu and B. Xu, *Angew. Chem., Int. Ed.*, 2014, **53**, 8104.
36 M. Reches and E. Gazit, *Science*, 2003, **300**, 625.
37 M. Gräber, W. Janczyk, B. Sperl, N. Elumalai, C. Kozany, F. Hausch, T. A. Holak and T. Berg, *ACS Chem. Biol.*, 2011, **6**, 1008.
38 W. Chan and P. White, *Fmoc solid phase peptide synthesis: a practical approach*, OUP, Oxford, 1999.
39 J. Montserat, L. Chen, D. S. Lawrence and Z.-Y. Zhang, *J. Biol. Chem.*, 1996, **271**, 7868.
40 I. W. Hamley, *Soft Matter*, 2011, **7**, 4122.
41 I. W. Hamley, A. Dehsorkhi, V. Castelletto, S. Furzeland, D. Atkins, J. Seitsonen and J. Ruokolainen, *Soft Matter*, 2013, **9**, 9290.
42 J. Shi, G. Fichman and J. P. Schneider, *Angew. Chem., Int. Ed.*, 2018, **57**, 11188.
43 D. Wu, N. Sinha, J. Lee, B. P. Sutherland, N. I. Halaszynski, Y. Tian, J. Caplan, H. V. Zhang, J. G. Saven, C. J. Kloxin and D. J. Pochan, *Nature*, 2019, **574**, 658.
44 F. Wang, O. Gnewou, S. Wang, T. Osinski, X. Zuo, E. H. Egelman and V. P. Conticello, *Matter*, 2021, DOI: 10.1016/j.matt.2021.06.037.

45 V. Castelletto, J. Seitsonen, J. Ruokolainen, C. Piras, R. Cramer, C. J. C. Edwards-Gayle and I. W. Hamley, *Chem. Commun.*, 2020, **56**, 11977.
46 K. Gayen, N. Nandi, K. S. Das, D. Hermida-Merino, I. W. Hamley and A. Banerjee, *Soft Matter*, 2020, **16**, 10106.
47 P. J. Jervis, C. Amorim, T. Pereira, J. A. Martins and P. M. T. Ferreira, *Soft Matter*, 2020, **16**, 10001.
48 Z. Liu, Y. Jiang, J. Jiang, D. Zhai, D. Wang and M. Liu, *Soft Matter*, 2020, **16**, 4115.
49 R. Yoshisaki, S. Kimura, M. Yokoya and M. Yamanaka, *Chem. – Asian J.*, 2021, **16**, 1937.